Table 1: Datasets used in this study

Experiment	**Radar/Ship**	**L (cm)**	V_{nyq} **(m/s)**	**# hours**	**Reference**
COARE	MIT/Vickers I	5	13.4	776	Short et al. 1997
	MIT/Vickers II	5	13.4	690	
	MIT/Vickers III	5	13.4	633	
TEPPS	NOAA/RHB	5	16.1	621	Yuter and Houze 2000
EPIC	NOAA/RHB	5	12.2	432	Raymond et al. 2004
LBA	TOGA	5	12.7	1244	Cifelli et al. 2002
KWAJALEIN	TRMM GV	10	25.6	4361	Schumacher & Houze 2000
JASMINE	NOAA/RHB	5	16.1	556	Webster et al. 2002
SCSMEX	CPOL/PRC5	5	13.2	529	Lau et al. 2000

* The Kwajalein data includes the KWAJEX data.

Table 2: Calibration of radar reflectivity

Experiment	**Radar**	**Offset (dBZ) GATE Z-R**	**Offset (dBZ) Local Z-R**	**Offset (dBZ) Previous studies**	**Reference**
COARE	MIT I	+0.2	+0.1	-2 - +12	Short et al. 1997
	MIT II	+7.2	+8.4	-2 - +12	
	MIT III	+6.9	+7.7	-2 - +12	
TEPPS	NOAA	+3.1	+5.2	+3.6	Nesbitt et al. 2003
EPIC	NOAA	-0.2	+2.3	0.0	Nesbitt et al. 2003
LBA	TOGA	+3.3	+4.9	+4.0	Nesbitt et al. 2003
KWAJALEIN	GV	+3.8	+4.7	+5	Yuter et al. 2004
JASMINE	NOAA	-2.4	N/A		
SCSMEX	CPOL	+2.5	N/A		

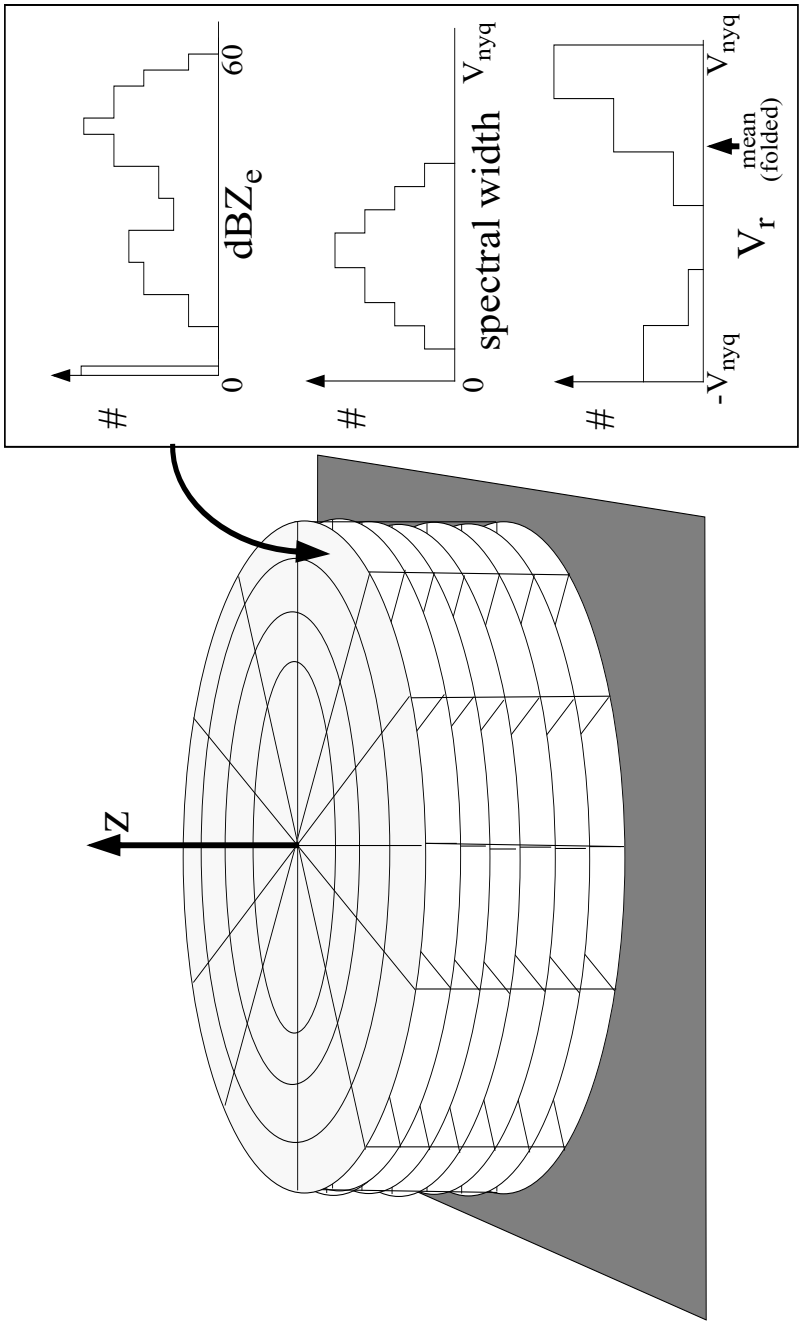

Figure 1: Schematic depiction of the cylindrical coordinate system, and the histograms in each space-time grid cell.

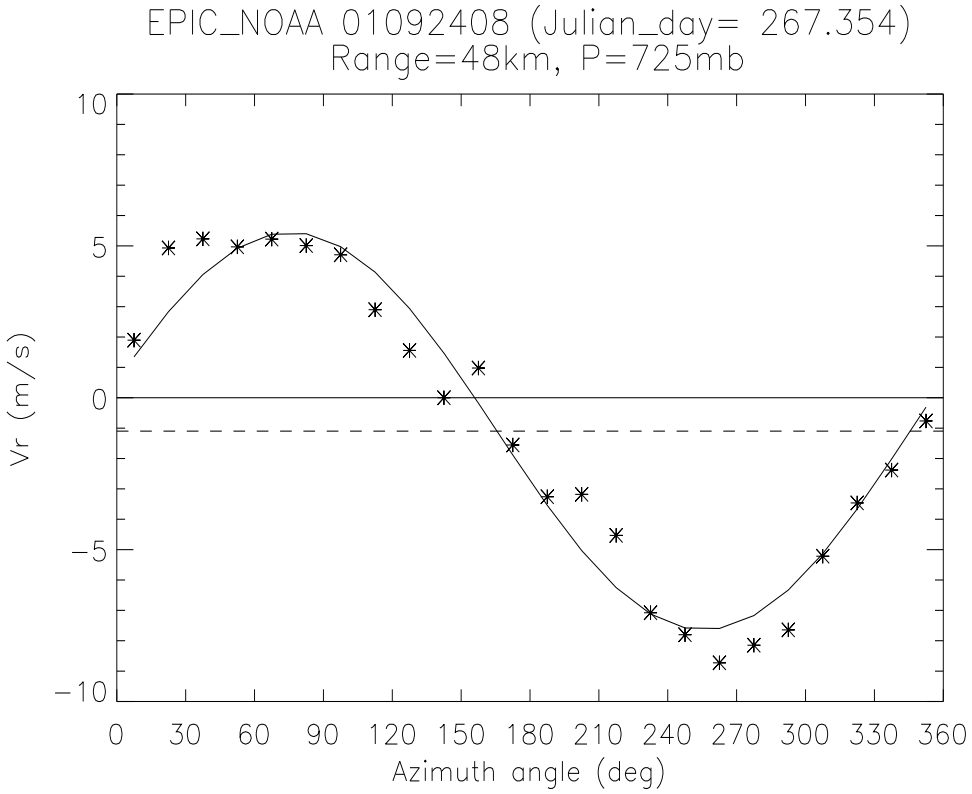

Figure 2: Radial velocity (stars) along 48 km range circle at 725 mb measured by shipborne radar during 0800-0900 UTC, 24 September 2001, during the EPIC project. The solid curve shows a fitted curve truncated at the first harmonic, and the dashed line shows its azimuthal mean.

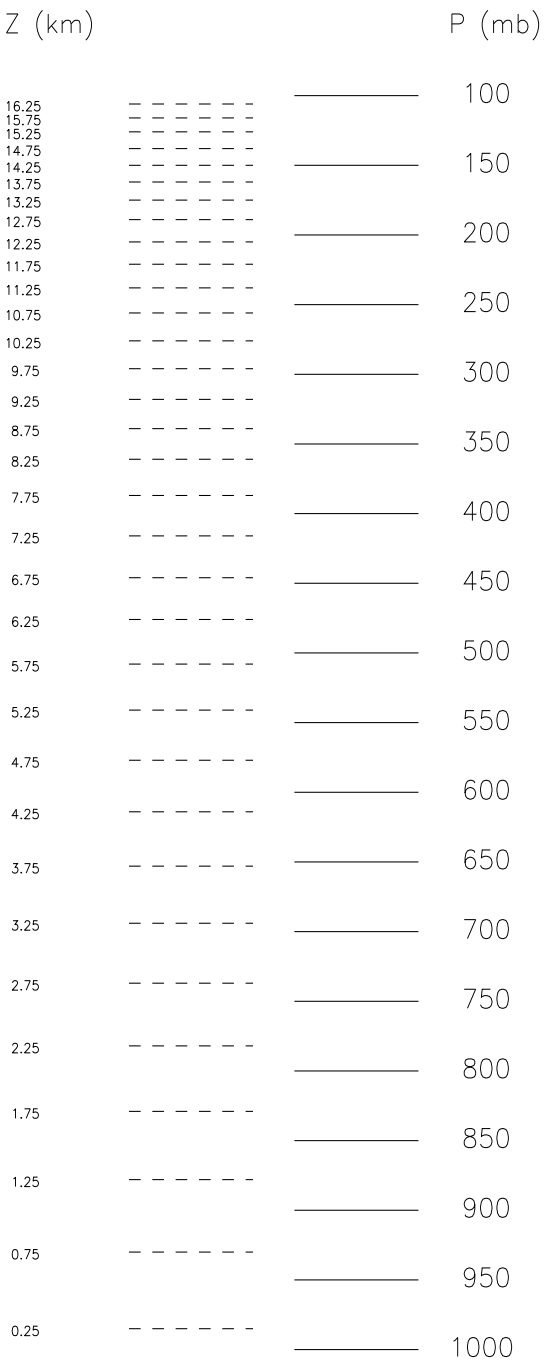

Figure 3: Height and pressure coordinates used in this study.

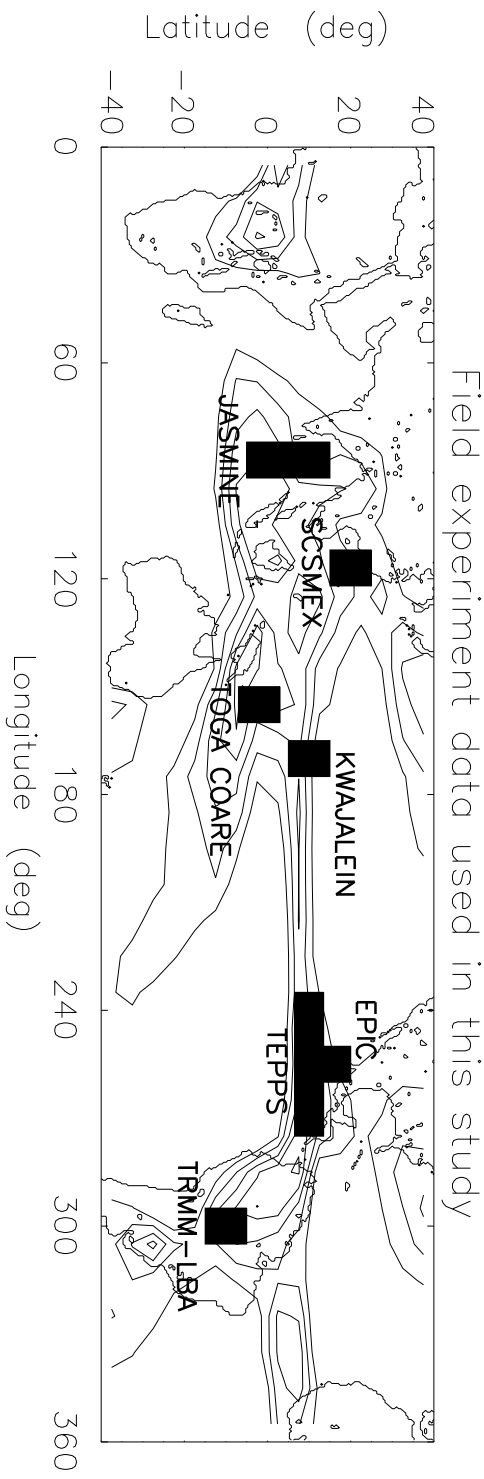

Figure 4: Locations of the field experiments whose data are used in this study.

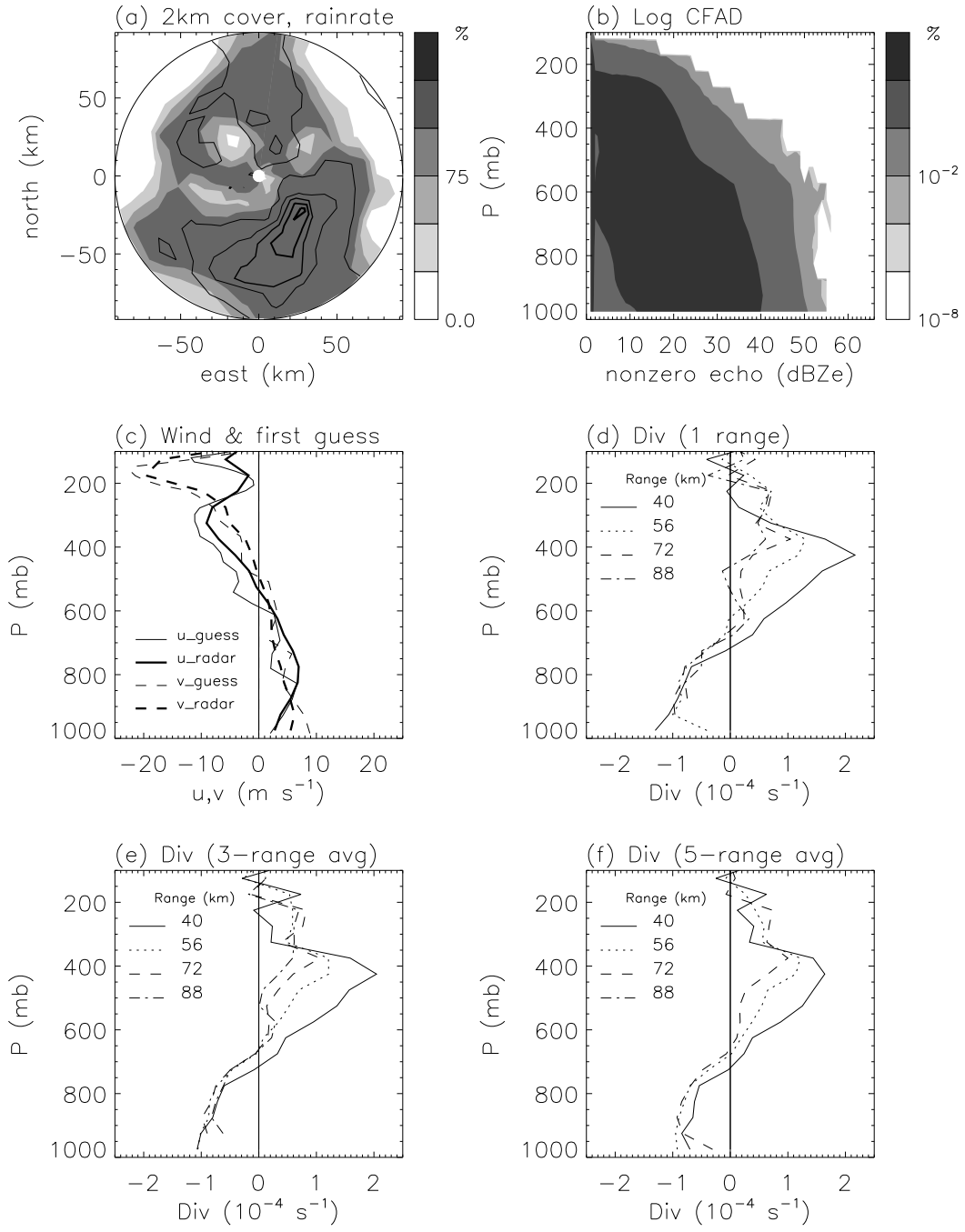

Figure 5: An example of the standard hourly data analysis product from the EPIC experiment at 08 UTC on 24 September, 2001 (Julian date 267.4). (a) A plan-view depiction of low-level echo. The filled contours are the fractional coverage by detectable echo during the hour, while open contours depict (with a nonlinear contour interval, proportional to the square root) estimated rainrate R. (b) A contoured frequency by altitude (CFAD, Yuter and Houze 1995) diagram summarizing the radar echoes within the 88 km range circle. At each altitude, the indicated frequency in all the 1dBZ bins sums to the total fractional cover by detectable ("nonzero") echo at that altitude. (c) Mean wind profiles including first guess zonal wind (thin solid) and meridional wind (thin dash), and radar zonal wind (thick solid) and meridional wind (thick dash). (d) Divergence profiles averaged over circles of indicated radii. (e) As in (d) except for 3-range pooled data. (f) As in (d) except for 5-range pooled data.

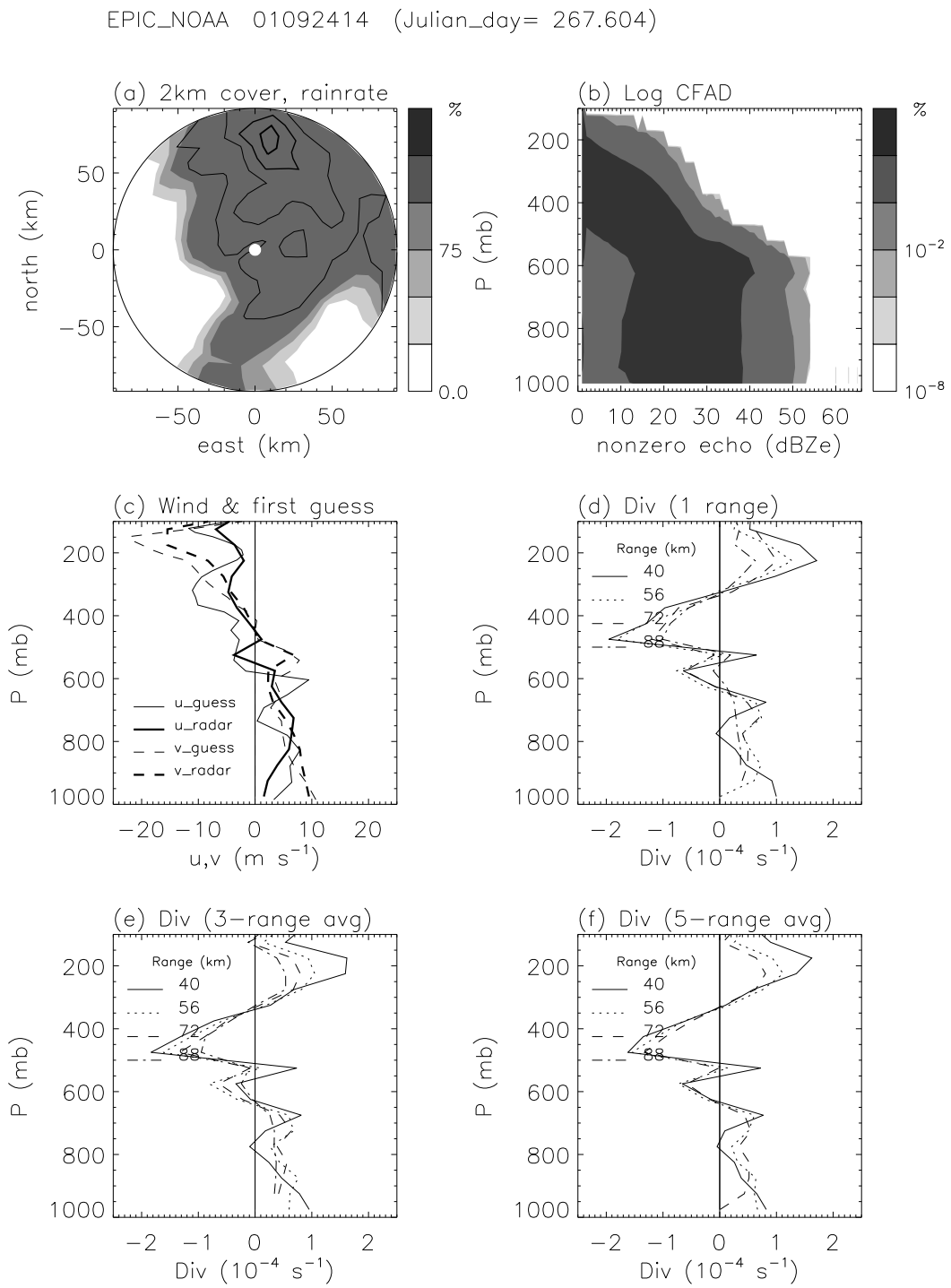

Figure 6: As in Fig. 5 except for 14 UTC on 24 September, 2001 (Julian date 267.6).

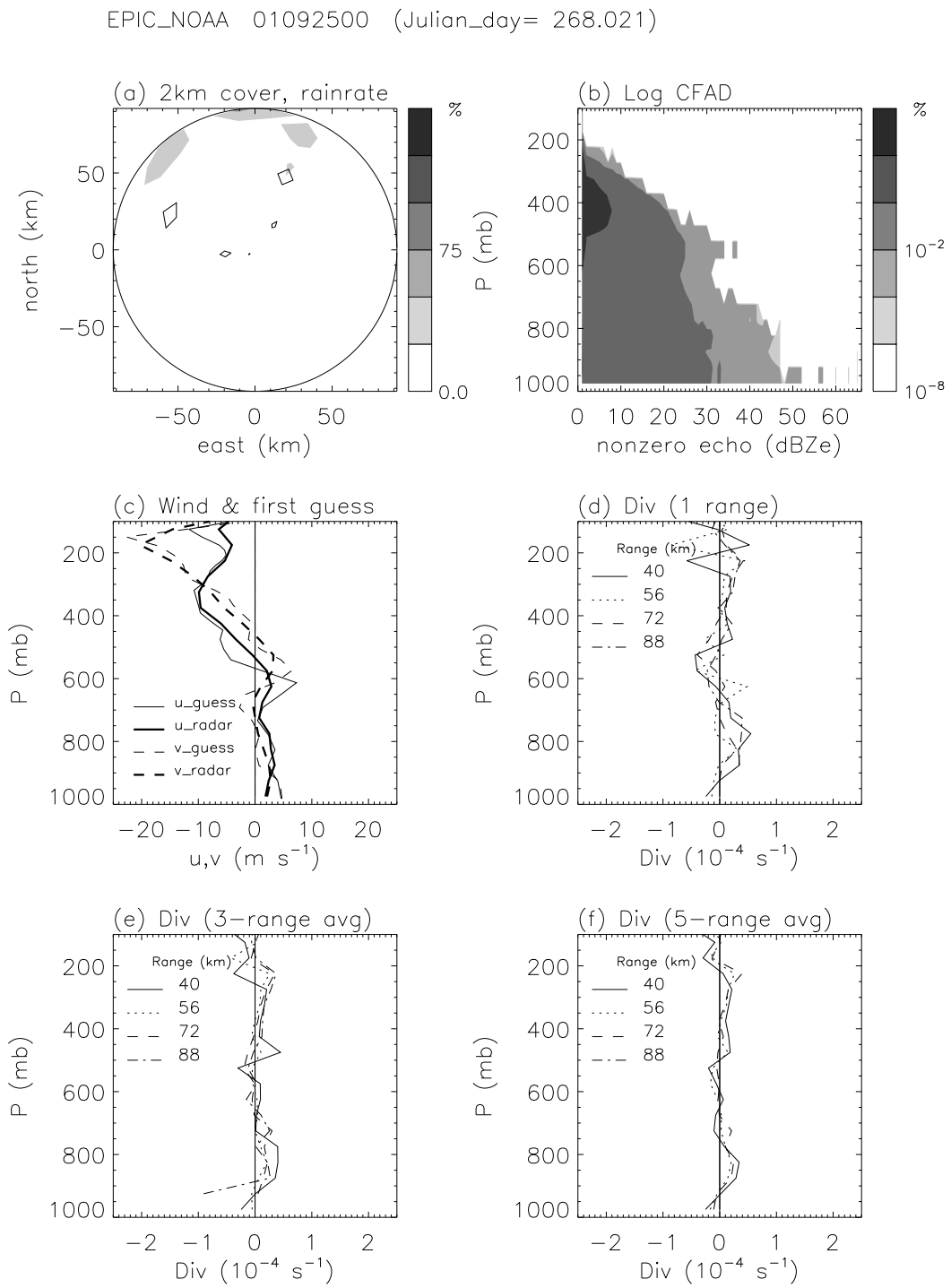

Figure 7: As in Fig. 5 except for 00 UTC on 25 September, 2001 (Julian date 268.0).

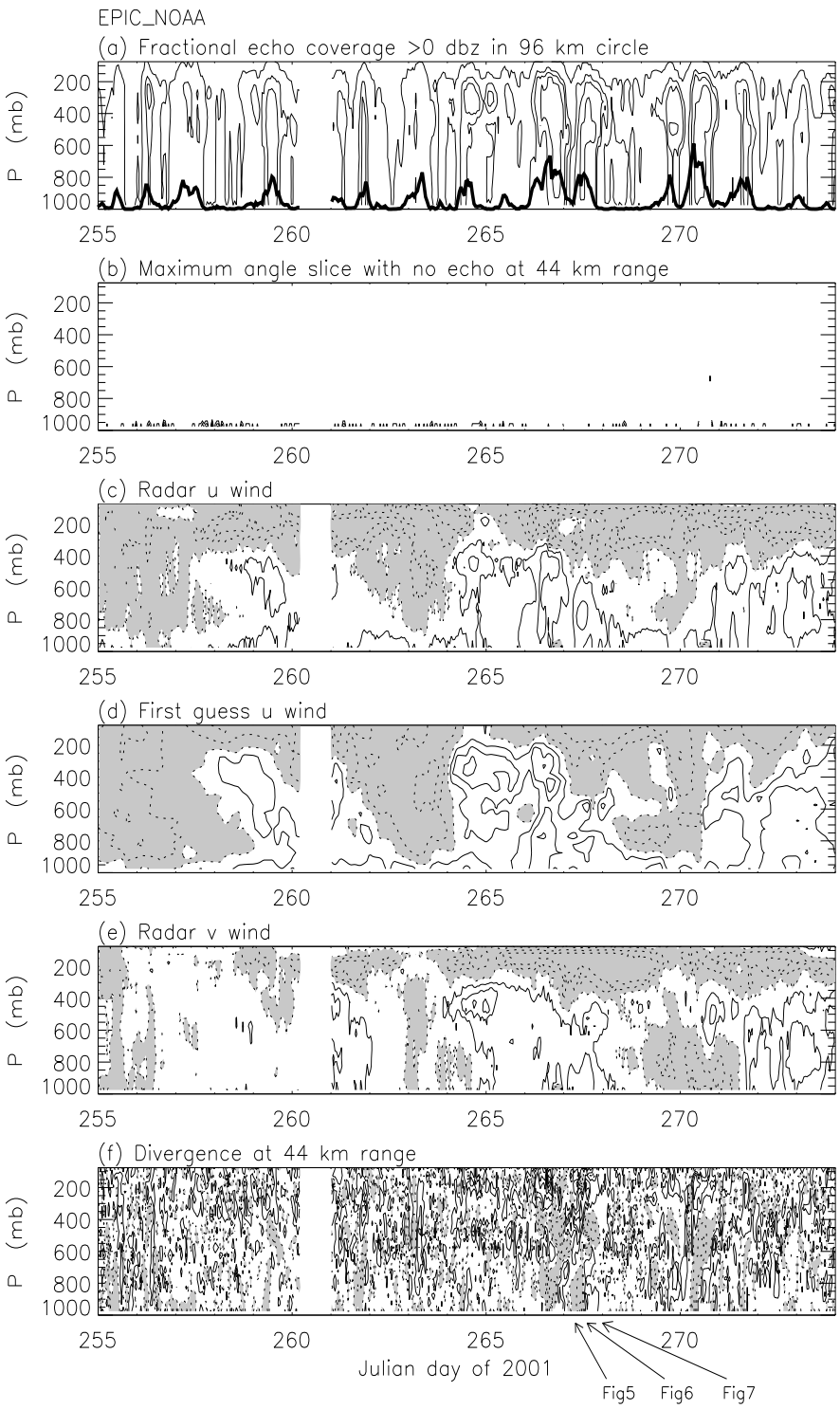

Figure 8: Time-height sections summarizing the EPIC 2001 radar data set. (a) Fractional coverage by detectable echo ¡ 96km from radar (contours: 1estimate (heavy curve, maximum value 6 mm h-1). (b) The maximum azimuth gap with no valid Doppler Vr estimates at 44 km range (contour: 30 degrees, essentially all of domain is less than that). (c) Radar zonal wind (contours +/- 2,6,10...m/s, negative dotted and shaded). (d) First guess zonal wind, contours as in (c). (e) Radar meridional wind, contours as in (c). (f) VAD divergence at 44 km range (contours +/- 25,75,125...x 10-6 s-1, negative dotted and shaded).

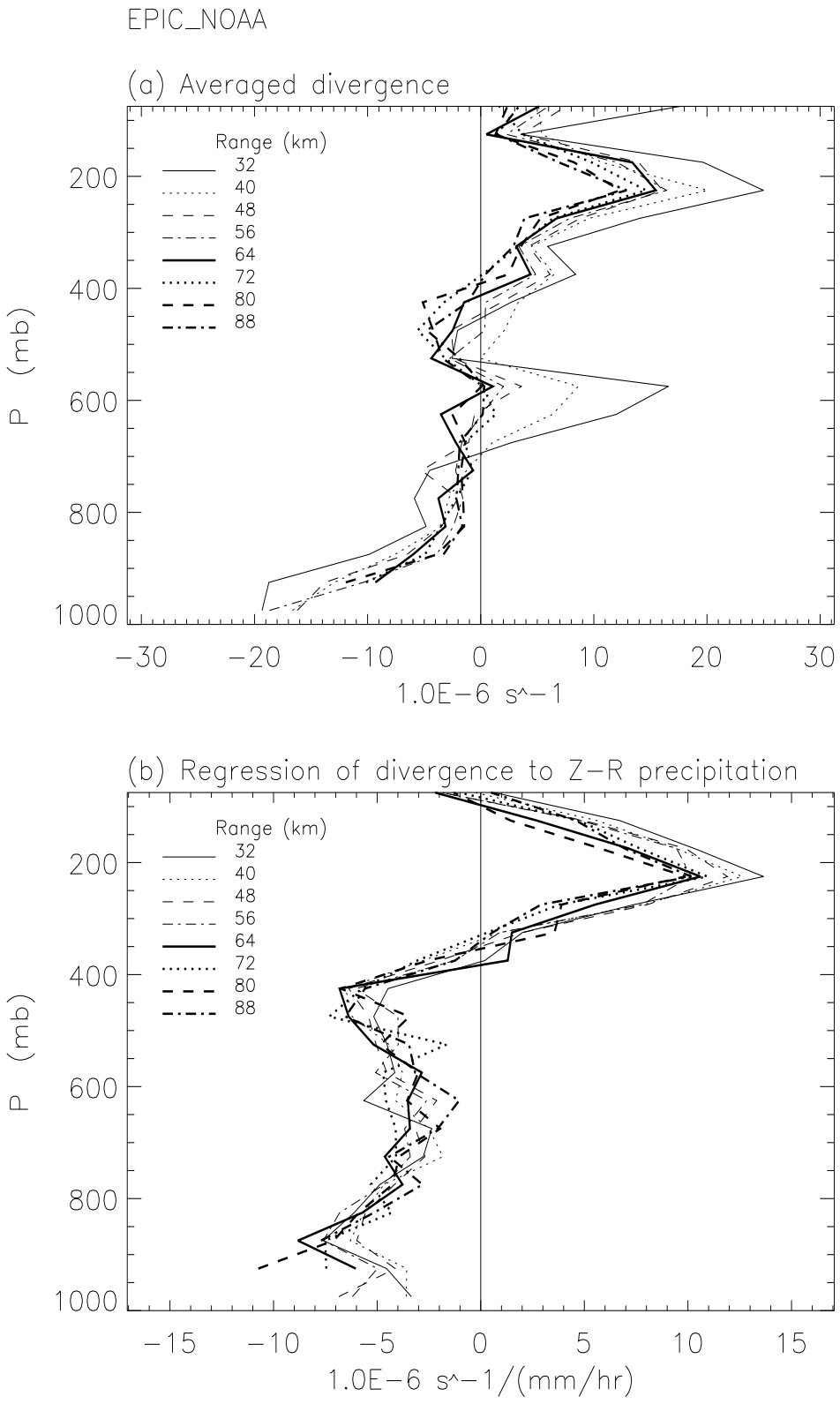

Figure 9: Statistics of 432 hours of data during the EPIC experiment. (a) Time-mean VAD-estimated divergence profiles. (b) Profiles of the linear regression coefficients relating divergence at each altitude to Z-R estimated near-surface precipitation.

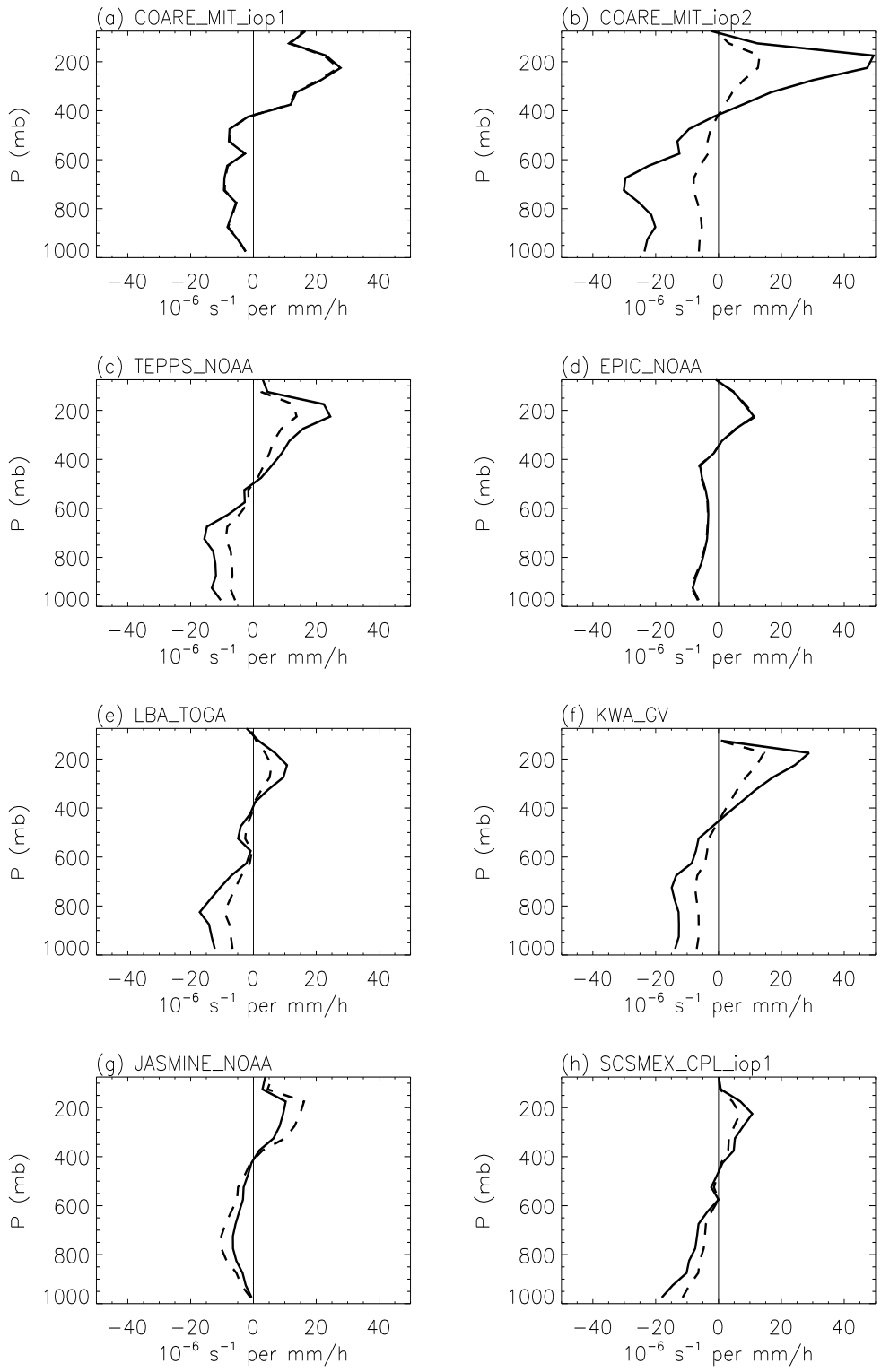

Figure 10: Profiles of the range-averaged linear regression coefficients relating divergence to Z-R estimated near-surface precipitation for (a) TOGA COARE, first deployment of the MIT radar aboard the R/V Vickers, (b) TOGA COARE, second MIT/Vickers deployment, (c) TEPPS, (d) EPIC, (e) LBA, (f) Kwajalein, (g) JASMINE, and (h) SCSMEX. The solid curves are with original reflectivity values, while dashed curves are after reflectivity correction (additive in dBZ) based on equating precipitation and moisture convergence estimates. Range averaging is a simple mean over the 8 ranges shown in Fig. 9.

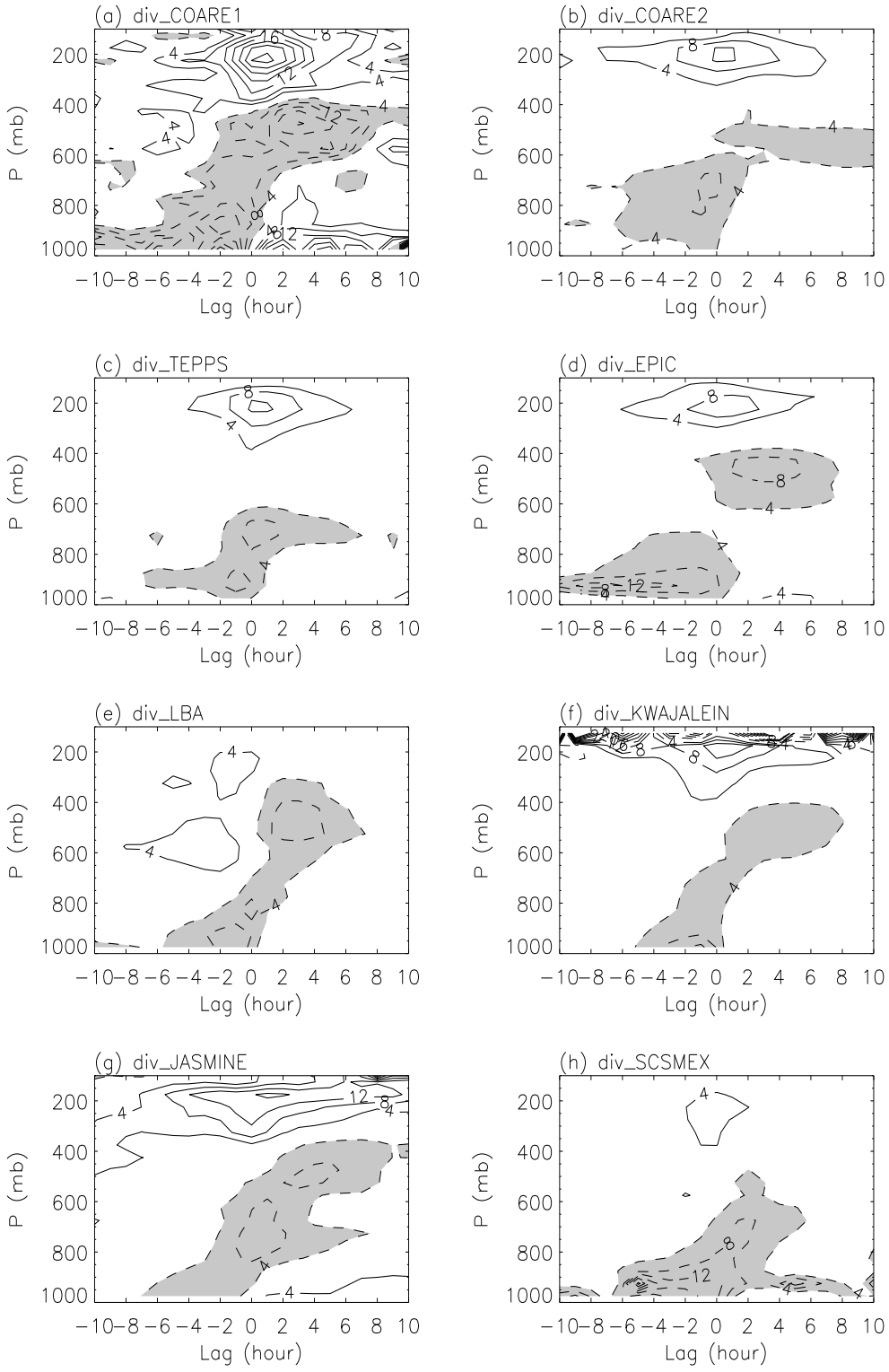

Figure 11: Range-averaged reflectivity-corrected regression coefficients, exactly like dashed curves in Fig. 10, but for different time lags of divergence with respect to precipitation.